ISSN 1023-1935, Russian Journal of Electrochemistry, 2008, Vol. 44, No. 11, pp. 1228–1239. © Pleiades Publishing, Ltd. 2008.
Original Russian Text © Yu.G. Chirkov, V.I. Rostokin, 2008, published in Elektrokhimiya, 2008, Vol. 44, No. 11, pp. 1321–1332.

Hydrogen–Oxygen (Air) Fuel Cell with Nafion and Platinum: Calculating Overall Characteristics, Comparing the Performance of a Cathode with Polymeric Electrolyte with a Hydrophobized Cathode with Liquid Electrolyte

Yu. G. Chirkov[a, z] and V. I. Rostokin[b]

[a]*Frumkin Institute of Physical Chemistry and Electrochemistry, Russian Academy of Sciences, Leninskii pr. 31, Moscow, 119071 Russia*

[b]*Moscow Institute of Engineering Physics, Kashirskoe Sh. 31, Moscow, 117409 Russia*

Received November 12, 2007

Abstract—Results of calculating the major overall characteristics of both an individual cathode and the whole hydrogen–oxygen (air) fuel cell with Nafion and platinum are shown. The effect of varying the parameters of both the active layer and the polymeric-electrolyte membrane on the overall characteristics of such a fuel cell is analyzed. The mechanisms of operation of active layers of hydrophobized cathodes and cathodes containing Nafion are compared. These two electrode types demonstrate a qualitative difference in the current generation mechanisms. As a result, the current in cathodes with Nafion increases more actively with the increase in overpotential (in proportion with $\mathrm{Exp}[\eta_0/2]$, where η_0 is the cathodic overpotential) as compared with the case of hydrophobized cathodes (here the current ~ $\mathrm{Exp}[\eta_0/4]$). This explains the fact that a fuel cell with Nafion demonstrates so high power characteristics as compared with a fuel cell with hydrophobized electrodes and liquid electrolyte.

Keywords: hydrogen–oxygen (air) fuel cell with Nafion and platinum, computer simulation of active layers of cathodes with solid polymeric electrolyte, hydrophobized electrode with liquid electrolyte

DOI: 10.1134/S1023193508110062

INTRODUCTION

Low-temperature (typical working temperature is 80°C) hydrogen–oxygen (air) fuel cells with solid polymeric electrolyte (Nafion) and platinum as the catalyst still remain among the major candidates for power sources in autonomous space and terrestrial units. Among their main advantages are the efficiency of chemical energy conversion into electricity, their high characteristics such as the power per weight unit (W/kg) and the power density (W/cm^2) [1].

Fuel cells with Nafion and platinum (and, the more so, cathodes as their most vulnerable parts) were the subject of quite a number of publications. However, from our viewpoint, no attempts were undertaken to explain why this system demonstrates so high characteristics (power density above 1 W/cm^2). In rare cases, an attempt was undertaken to calculate the major overall characteristics of active layers of cathodes based on Nafion and platinum [2–8]. This is why, their current generation mechanism still remains unclear and no studies are known to compare the electrodes with Nafion with the other types of electrodes.

Computer simulation of active layers with polymeric electrolyte was carried out in a series of studies [9–12]. A "model of equidimensional grains" (where grains represent agglomerates of the carrier and platinum particles and agglomerates of Nafion particles), suitable for calculating the effective coefficients (oxygen diffusion, protonic conductivity) and overall characteristics of cathodes with Nafion and platinum was put forward [9]. Within the framework of this model, the characteristic specific current density in such cathodes was calculated [10], the effect of Nafion concentration in the active layer on the cathode overall characteristics were analyzed [11], and it was shown how the working thickness of an active layer should be chosen [12]. However, the central problem remains so far unsolved, namely, it was not shown that the calculated overall currents and powers densities correspond to those observed experimentally. This gap will be filled in the present study.

The further steps can be undertaken only after we are convinced that the "model of equidimensional grains" correctly describes the peculiarities of operation of cathodes with polymeric electrolytes. Then, it will be reasonable to compare the mechanism of operation of a cathode with Nafion with a sufficiently well

[z] Corresponding author: olga.nedelin@gmail.com (Yu.G. Chirkov).

studied and described mechanism of operation of hydrophibized cathodes with liquid electrolytes (the computer simulation of this system and an example of calculations of its overall characteristics are given in [13]). Such a comparison is the second goal of this study and will help us to explain why the current generation processes proceed the most effectively precisely in cathodes with polymeric electrolytes.

PARAMETERS OF AN ACTIVE LAYER OF A CATHODE WITH NAFION AND PLATINUM

The problem of comparing the results of computer (model) and real experiments is by no means easy. Hence, for this problem to be solved, it is necessary not only to compare the experimental and theoretical overall characteristics of this cathode but also to experimentally find many parameters of the cathode chosen for studies, namely, the parameters involved in the "model of equidimensional grains". However, the number of required parameters is very large, namely, over several tens.

For instance, it is necessary to know the sizes of Nafion and carrier grains, their volume concentrations, the active layer fraction accounted for voids, the steady-state potential, the exchange current, the fraction of the platinum specific surface that can be involved in the electrochemical process, the effective values of oxygen diffusion coefficient and protonic conductivity, the active layer thickness, etc. It is rather difficult to find them experimentally. The reverse problem, to theoretically find the parameters involved in the "model of equidimensional grains", is also difficult. However, this must be done because without this it is impossible to calculate the overall characteristics of a cathode and the whole fuel cell with polymeric electrolyte.

The parameters necessary for carrying out the calculations are apparently divided into groups of values that characterize (1) the external conditions at which a fuel cell operates, (2) the electrochemical process of oxygen reduction on platinum, (3) the active layer structure, and (4) the real and effective coefficients characterizing the mass and electricity transfer.

External parameters involve the working temperature of a fuel cell t, the pressure in the gas chamber p^*, the cathode active layer thickness Δ, and the membrane thickness δ.

Parameters of electrochemical kinetics. Oxygen reduction on platinum in acidic media is characterized by the presence of two Tafel slopes, namely, 60 mV (high potential range) and 120 mV (low potential range) [14–17]. The procedure of calculating overall currents and other active layer characteristics for cathodes with Nafion and platinum in the cases where the Tafel plot has several segments with different slopes is shown in [18].

Let us choose E-TEK (XS72 + 20 mass % Pt) as assume that $E_{st} = 1.05$ V is the steady-state potential and $E^* = 0.875$ V is the potential at which the Tafel slope changes. The Tafel plot slopes are $b_1 = (6/2.3) \times 10^{-2} = 2.6 \times 10^{-2}$ V and $b_2 = (12/2.3) \times 10^{-2} = 5.2 \times 10^{-2}$ V. Assume that at $t = 50°C$, the exchange current $i_0 = 10^{-8}$ A/cm^2 [19]. According to the temperature dependence of the exchange current of oxygen reduction on platinum shown in [20], $i_0 = 2.27 \times 10^{-8}$, 1.01×10^{-7}, and 1.80×10^{-7} A/cm^2 for $t = 60$, 80, and 95°C, respectively.

Parameters of the active layer structure. It is conventionally assumed [21] that the size of individual carbon black particles is ≈20–40 nm, the size of agglomerates of carbon black particles (carrier grains) vary from several tens to several hundred nm, the pores between these agglomerates are in the same range of sizes being partly filled with agglomerates of solid polymeric electrolyte molecules (Nafion grains).

Let us assume that the active layer structure can be described by the "model of equidimensional grains" and choose the optimum active layer structure. This means that the active layer lacks voids and the volume concentrations of the Nafion and carrier grains are equal to one another $g_e = g_s = 0.5$. We assume that the grain size $d = 100$ nm, the size of pores in carrier grains $d_s = 30$ nm, the porosity of carrier grains $\nu = 0.5$.

Effective coefficients. As was shown in [10], the equations used in calculating the overall characteristics of a cathode with Nafion involve the following four parameters: effective diffusion coefficient of oxygen D^*, effective specific conductivity of protons k^*, oxygen solubility in Nafion c_0, and the characteristic bulk current density i^*. According to model calculations [9, 11], in an active layer with the condition $g_e = g_s = 0.5$ fulfilled, the effective diffusion coefficient of oxygen $D^* = 4.5 \times 10^{-4}$ cm^2/s, the effective specific protonic conductivity $k^* = 1.09 \times 10^{-2}\ \Omega^{-1}$ cm^{-1} (for the optimal specific conductivity of Nafion $k = 0.1\ \Omega^{-1}$ cm^{-1}, the specific conductivity of Nafion within the membrane k_1 is also assumed equal to 0.1 Ω^{-1} cm^{-1}).

Next, we assume that the oxygen solubility in Nafion, which depends on pressure according to the Henry law, at a pressure $p^* = 101$ kPa is equal to $c_0 = 5 \times 10^{-6}$ g-mol/cm^3 [22]. Then, under pressure, e.g., $p^* = 505$ kPa, the solubility $c_0 = 2.5 \times 10^{-5}$ g-mol/cm^3.

Now, it remains to determine the characteristic bulk current density i^*. The latter should be equal to the exchange current i_0 times the fraction of the specific (per volume unit of the cathode active layer) surface S of catalyst (platinum) particles that is accessible for the catalysis and involved in the electrochemical process. Thus,

$$i^* = i_0 S. \quad (1)$$

In a cathode with Nafion, the electrochemical process can proceed only in the sites where a grain involved in an ionic cluster (proton supplier) is in direct contact with the gas cluster (electron and oxygen supplier). In the "model of equidimensional grains"

(microcubes with the edge length d), the maximum contact surface at the encounter of two clusters mentioned above is calculated according to the following formula [9, 11]:

$$S^* = 1.33/d. \quad (2)$$

Naturally, the specific surfaces S and S^* are not identical. Estimating the surface S requires taking into account several factors. First, as was mentioned above, a real active layer consists of non-identical grains. There is a size distribution of grains. This is why in our calculations, d was assumed equal to its intermediate value (between tens and hundreds of nm) of 100 nm.

Second, the surface of contact between grains involved in the ionic and gas clusters is not indeed ideally smooth. Actually, there exists a thin transition region in which carbon black particles are mixed with the Nafion molecules. Hence, the real specific surface of platinum involved in the electrocatalysis should exceed S^* being equal to $S^*\xi$, where parameter $\xi > 1$. The surface of contact between clusters seems to be "diffuse" to a certain "depth", which should be taken into account when calculating S.

Third, it also should be taken into account that catalyst grains do not cover the whole "diffuse" surface of the contact between a ionic and a gas cluster. The specific density of platinum exceeds the carrier (carbon black) density by an order of magnitude; hence, only a small fraction of the external surface of carrier grains is catalytically active. Hence, it seems reasonable to calculate S using the formula

$$S = S^*\xi\mu, \quad (3)$$

where the term $\mu < 1$ is the "electrochemical roughness factor" introduced in [10]. This value can be considered as simply a fraction of the carrier surface $S^*\xi$ that is covered with platinum particles.

Now, we determine μ. Obviously, this quantity increases with the platinum content in carrier grains g_w. Platinum particles are considered as microcubes with the edge length d_P. Being packed uniformly and compactly on the carrier external surface, these microcubes produce a catalyst layer of a thickness τ (dimensionless value). As was shown in [10], if the average size of carrier (carbon black) particles $d \gg d_P$, the average size of platinum particles, as was experimentally observed [21], then the relationship between the μ and τ takes the following form:

$$\mu = 3.845\tau. \quad (4)$$

Now, it remains to relate τ to the platinum content in the carrier grains g_w. Since by definition

$$g_w = V_P\rho_P/(V_P\rho_P + V_s\rho_s), \quad (5)$$

where V_P, V_s are specific volumes and ρ_P, ρ_s are the densities of platinum and carbon black, then in view of obvious relationships,

$$V_s = d^3, \quad (6)$$

$$V_P = 6d^2d_P\tau. \quad (7)$$

The latter two formulas should be substituted into Eq. (5). Then, taking into account Eq. (4), we ultimately obtain

$$\mu = 3.845(\rho_s/\rho_P)(d/6d_P)[g_w/(1 - g_w)]. \quad (8)$$

Now, we pass to estimates. Assume that $\rho_s = 1.8$ g cm^{-3}, $\rho_p = 21.5$ g cm^{-3}, $d = 30$ nm, $d_P = 2$ nm, $g_w = 20$ mass %, then $\mu = 0.2$. For parameter [xi], we take a value $\xi = 5.0$. Hence, the specific surface of platinum accessible for electrocatalysis in active layer volume unit $S = 1.33 \times 10^5$cm^{-1}. Next, using Eq. (1), we find that in the high potential range, the temperatures of 60, 80, and 95°C correspond to the following bulk current densities i^*, A/cm^3: 3.02×10^{-3}, 1.34×10^{-2}, and 3.72×10^{-2}, respectively.

CALCULATING OVERALL CHARACTERISTICS OF H_2–O_2 (AIR) FUEL CELLS WITH NAFION ANF PLATINUM

Now, we embark on estimating the overall characteristics of the cathode and the whole hydrogen–oxygen (air) fuel cell and analyzing how they depend on variations in the main parameters of both the active layer and the membrane of a solid polymeric electrolyte. The main parameters include the fuel cell temperature t, the pressure in the gas chamber p^*, the active layer thickness Δ, and the Nafion membrane thickness δ.

Figure 1 shows the results of calculating the voltammetric curves of an oxygen cathode and the dependences of the power density of an hydrogen–oxygen fuel cell with Nafion and platinum on the overall current for the gas-chamber pressure values of 101 (Fig. 1a) and 505 kPa (Fig. 1b). The fuel cell temperature took three values, 60, 80, and 95°C. The active layer thickness $\Delta = 10$ μm.

Comparing Figs. 1a and 1b shows that as the temperature and pressure increase, the overall current and the power density substantially increase. The pressure effect is associated with the fact that the characteristic diffusion current $I_d^0 \sim (c_o)^{1/2}$, i.e., proportional to the square root of oxygen solubility in Nafion c_o and, hence, to the square root of the gas pressure in the chamber p^*.

Figure 1 confirms that our choice of parameters is right, and the "model of equidimensional grains" adequately describes the processes that occur in real oxygen cathodes with Nafion and platinum. Indeed, the best experimental voltammetric curves available in the literature demonstrate the overall current of about 1 A/cm^2 for a platinum concentration on the carrier $g_w = 20$ mass %, at a pressure $p^* = 505$ kPa, $t = 95$°C, and the potential $E_0 = 0.7$ V [23]. In Fig. 2b too, at $E_0 = 0.7$ V, the overall current $I = 1.18$ A/cm^2 and the power density of a hydrogen–oxygen fuel cell $W = 0.825$ W/cm^2.

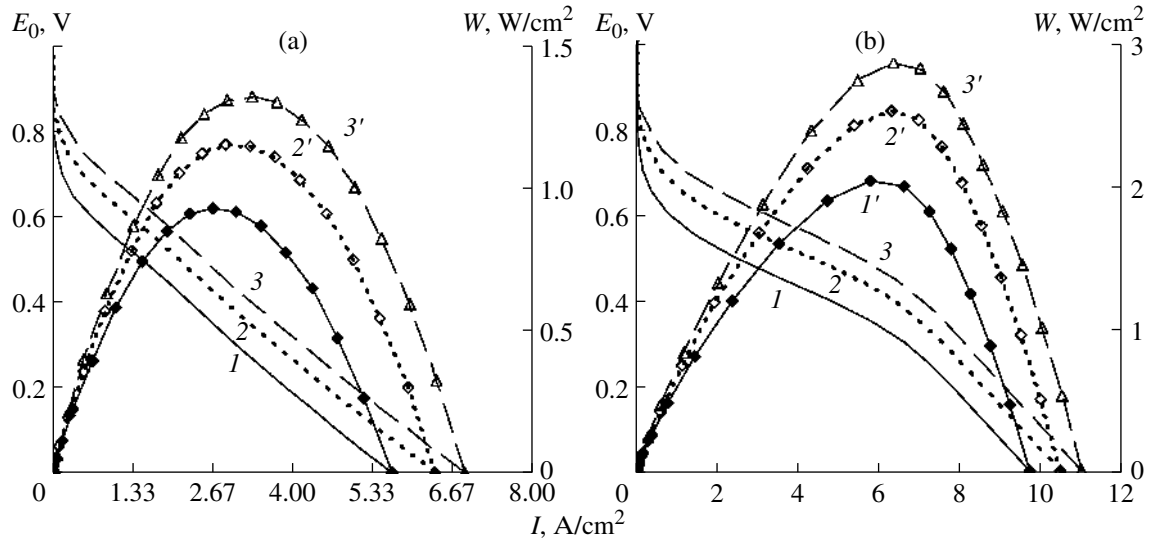

Fig. 1. (*1–3*) Voltammetric curves of an oxygen cathode and *(*1*'–*3*') dependences of the power density of a hydrogen–oxygen fuel cell on the overall current. p*, kPa: (a) 101 and (b) 505°C; (*1*, *1*') 60, (*2*, *2*') 80, and (*3, 3*`) 95°C. *3*, *3*' – 95°C. Δ = 10 μm, g_w = 20 mass %, δ = 0.

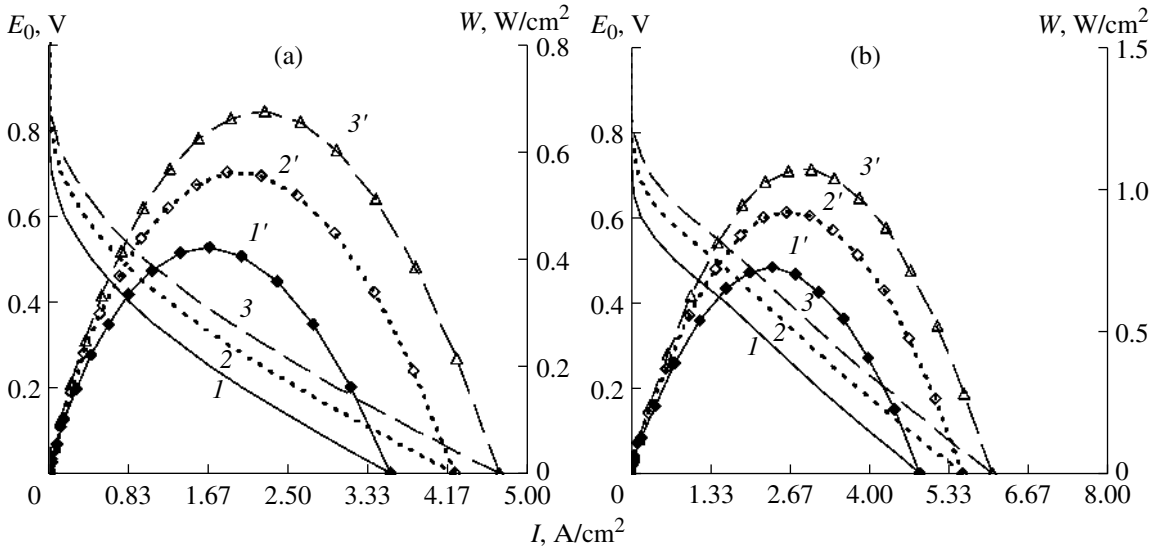

Fig. 2. (*1–3*) Voltammetric curves of an air cathode and *(*1*'–*3*') dependences of the power density of a hydrogen–air fuel cell on the overall current. p*, kPa: (a) 101 and (b) 505; (*1, 1*`) 60, (*2, 2*`) 80, and (*3, 3*`) 95°C. Δ = 10 μm, g_w = 20 mass %, δ = 0.

Furthermore, note that as the potential of a hydrogen–oxygen fuel cell decreases, its current and power rapidly increase. In Fig. 1b at E_0 = 0.6 V, the current I = 3.1 A/cm^2, the power density W = 1.85 W/cm^2. For E_0 = 0.5 V, the current I = 5.4 A/cm^2, the power density W = 2.7 W/cm^2.

Figure 2 illustrates calculations of the same characteristics as in Fig. 1 but for a hydrogen–air fuel cell in place of the hydrogen–oxygen cell. A comparison of Figs. 1 and 2 shows that the changeover of fuel cells from the oxygen to air type leads to an approximately 2-fold decrease in the overall current. This is associated with the fact that on the back surface of cathode's active layer (at its boundary with the gas-diffusion layer, GDL), the supersaturation of Nafion with oxygen $\acute{c}$ = 1 in an oxygen cathode and $\acute{c}$ = 0.2 in an air cathode, i.e., differs by a factor of 5. In Fig. 2b (for p* = 505 kPa and t = 95°C), at the air cathode potential E_0 = 0.7 V, the overall current I = 0.34 A/cm^2, the power density W = 0.24 W/cm^2. For E_0 = 0.6 V, the current I = 1.04 A/cm^2, the power density W = 0.62 W/cm^2. For

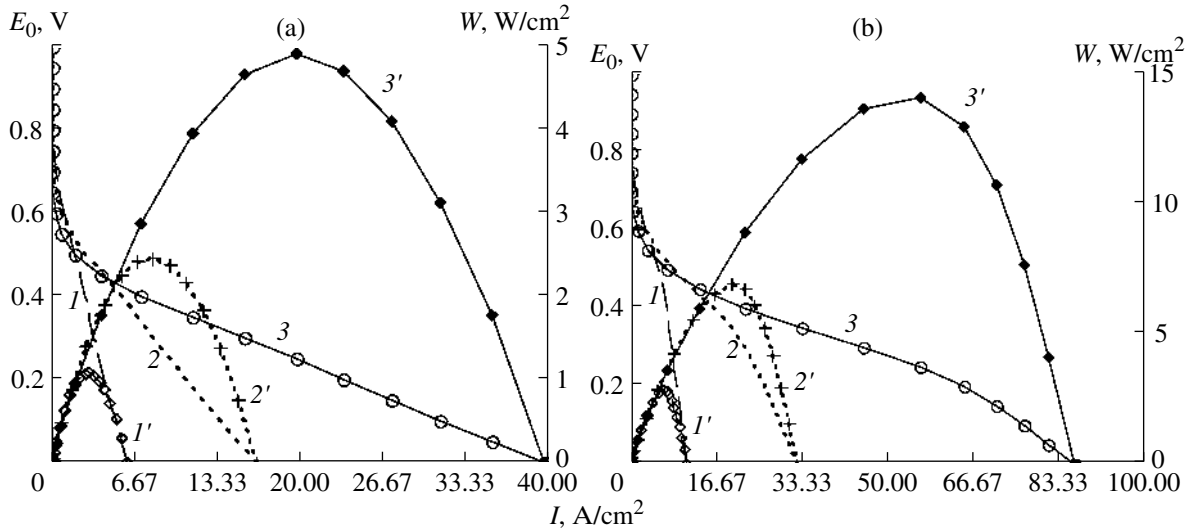

Fig. 3. (*1–3*) Voltammetric curves of (a) air and (b) oxygen cathodes and *(*1*'–*3*') dependences of the power density of (a) hydrogen–air and (b) hydrogen–oxygen fuel cells on the overall current. t = 95°C; p^* = 505 kPa, Δ, μm: (*1*, *1*') 10, (*2*, *2*') 3, and (*3*, *3*') 1; g_w = 20 mass %, δ = 0.

E_0 = 0.5 V, the current I = 1.88 A/cm^2, the power density W = 0.94 W/cm^2.

Now, we analyze how the overall characteristics depend on the cathode active layer thickness. Figure 3 shows the results of calculating the voltammetric currents of the air (Fig. 3a) and oxygen (Fig. 3b) cathodes with Nafion and platinum and the dependences of the power density of the corresponding fuel cells on the overall current. The fuel cell temperature t = 95°C, the gas-chamber pressure p^* = 505 kPa, and the cathode active layer thickness Δ was 10, 3, and 1 μm.

Attention is drawn to the fact that in the range of high cathoding potentials, approximately at $E_0 > 0.5$ V, cathodes with thicker active layers have better characteristics than cathodes with thin active layers. Thus at potential E_0 = 0.7 V (Fig. 3b), for an oxygen cathode, we have the following overall currents (A/cm^2) and power densities (W/cm^2): I = 1.18 and W = 0.825 for Δ = 10 μm, I = 0.63 and W = 0.44 for Δ= 3 μm, and I = 0.23 and W = 0.16 for Δ = 1 μm. Similarly, for an air cathode (Fig. 3a), the characteristics are as follows: I = 0.34 and W = 0.24 for Δ = 10 μm, I = 0.14 and W = 0.095 for Δ = 3 μm, and I = 0.05 and W = 0.03 for Δ = 1 μm. The overall current linearly increases as Δ increases from 1 to 3 μm. Its growth slightly decelerates only at Δ = 10 μm.

On the other hand, in the low potential range, preference should be given to cathodes with thin active layers. Thus in an oxygen cathode at a potential E_0 = 0.4 V (Fig. 3b), the overall currents (A/cm^2) and power densities (W/cm^2) are as follows: I = 7.01 and W = 2.8 for Δ = 10 μm, I = 16.27 and W = 6.51 for Δ = 3 μm, and I = 22.19 and W = 8.88 for Δ = 1 μm. In an air cathode at E_0 = 0.4 V (Fig. 3a), the currents (A/cm^2) and powers (W/cm^2) are as follows: I = 2.65 and W = 1.06 for Δ = 10 μm, I = 5.58 and W = 2.23 for Δ= μm, and I = 7.17 and W = 2.87 for Δ = 1 μm.

Summarizing, in place of the power density of an individual cathode (up to now we assumed the thickness of a Nafion membrane δ = 0), we estimate the power density of a whole fuel cell with Nafion and platinum (in this study, for simplicity sake, we assume the hydrogen overpotential to be equal zero). Figure 4 shows the results of calculations for oxygen cathodes with the active layer thickness values of 10 and 1 μm and several Nafion membrane thicknesses from 0 to 25 μm (a hydrogen–oxygen fuel cell with Nafion and platinum at t = 95°C, g_w = 20 mass %, p^* = 505 kP).

Taking into account the Ohmic limitation in the membrane leads to the lower power density of a fuel cell. The data in Fig. 4 show that if the membrane and the cathode active layer have comparable thicknesses (δ ~ Δ), the Ohmic losses in the membrane can be neglected. Assuming δ = 10 μm (in Fi. 4a) and δ = 1 μm (in Fig. 4b), we obtain the following values for power density. In Fig. 4a, the power density W = 0.81, 1.76, and 2.42 W/cm^2 for the cathode potentials E_0 = 0.7 V, 0.6, and 0,4 V, respectively. In Fig. 4b, the power density W = 0.16, 0.88, and 3.52 W/cm^2 at E_0 = 0.7, 0.6, and 0.5 V, respectively.

It deserves mentioning that the progress in the development of fuel cells with polymeric electrolytes is fast and occurs by several directions. Thus there is a trend towards decreasing the Nafion membrane thickness. The membrane thickness progressively decreased from 175/125 μm (Nafion 117/115) [24] to 25 μm [25–27]. The active layer thickness was also progressively decreased, namely, from 100 μm [28] to 10 μm and

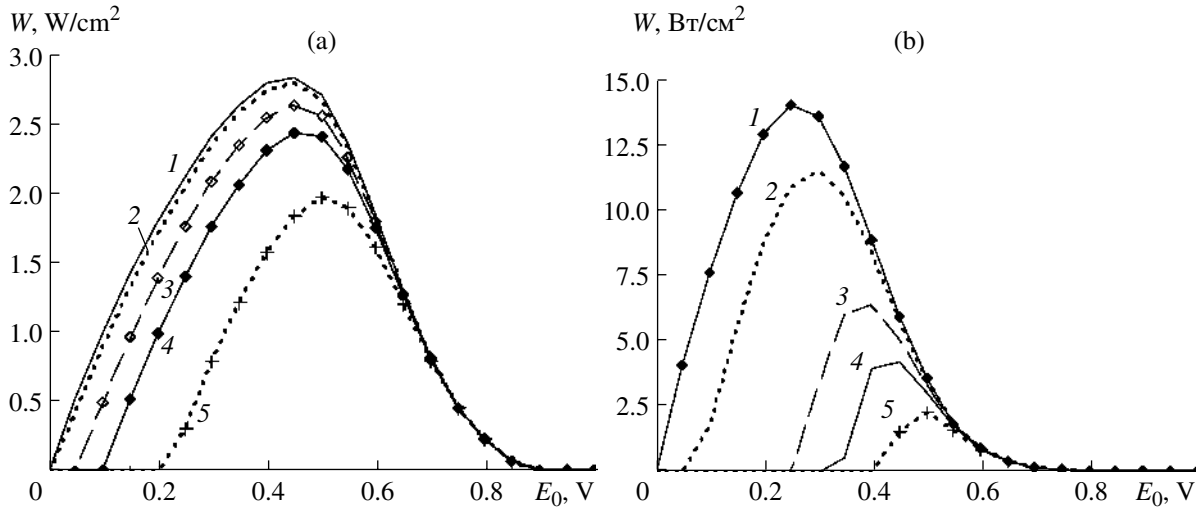

Fig. 4. Dependences of the power density of a hydrogen–oxygen fuel cell with Nafion and platinum on the cathodic potential for Δ, μm: (a) 10, (b) 1. δ, μm: (*1*) 0, (*2*) 1, (*3*) 5, (*4*) 10, (*5*) 25. t = 95°C, g_w = 20 mass %, p^* = 505 kPa.

lower. An important advantage of thin active layers lies in the fact that they contain smaller amounts of expensive platinum-group catalysts as compared with thick active layers. Thus the thicknesses of Nafion membranes δ and active layers Δ we used in our calculations should not appear extreme.

Thus, we have shown that the results of calculations of overall characteristics of hydrogen–oxygen (air) fuel cells with Nafion and platinum, carried out in the framework of the "model of equidimensional grains", are commensurable with those observed experimentally. Thus, the "model of equidimensional grains" can correctly describe the peculiarities of the mechanism of operation of cathodes with polymeric electrolytes. This model can also be used in comparing the cathodes with polymeric electrolytes and the hydrophobized cathodes with liquid electrolyte.

COMPARING MECHANISMS OF OPERATION OF ACTIVE LAYERS OF HYDROPHOBIZED ELECTRODES AND THOSE CONTAINING NAFION

Let us consider Figure 5. This figure illustrates the active layers of a hydrophobized cathode (Fig. 5a) and a cathode with Nafion (Fig, 2b) within the framework of the "model of equidimensional grains" (as will be shown below, the same model but in the different context allowed the computer simulation of active layers of hydrophobized cathodes with liquid electrolytes to be carried out [13]). The figure also shows the routes (channels) in both type of cathodes for the components involved in the electrochemical process, namely electrons (e), protons (H^+), and oxygen molecules (O_2). Figure 5c presents the schematic illustrations of the structure of all grains in hydrophobized cathodes and cathodes with Nafion. In the following text, for the simplicity sake, we assume that the active layers contain no voids (the desirability of this assumption was substantiated in [9, 11]).

Now, we explain the following designations introduced in Fig. 5: M is the electrolyte chamber (hydrophobized cathode) or membrane (of Nafion) in a fuel cell, AL are active layers, GDL are gas-diffusion layers, CG are carrier (carbon black) grains with platinum catalyst, PG are PTFE grains, PEG are polymeric electrolyte grains, CB are carbon black particles, Cat are catalyst particles, PF are PTFE particles, PEM are polymeric electrolytes molecules.

In Fig. 5, each grain represents a microcube with the edge length d. Indeed, when operating with the "model of equidimensional grains" it should be remembered that the true picture of the distribution of CG and PG in a hydrophobized electrode (Fig. 5a) and also of CG and PEG in an electrode with Nafion (Fig. 5b) is more complicated, three-dimensional, and determined by the active layer composition (concentrations of its components). Moreover, there indeed exists a distribution of all grains over sizes and shapes, because the parameter d represents an average value of grain sizes.

One and the same CG (in Figs. 5a and 5b, they are shaded) are used in both types of cathodes. However, in a hydrophobized cathode, the CG pores (Fig. 5c) are filled with liquid electrolyte and the catalyst is throughout wetted with it. A different picture is observed for a cathode with Nafion. For the optimum Nafion wetting, when the specific protonic conductivity is the maximum and reaches $k = 1 \times 10^{-1}$ Ω^{-1} cm^{-1} [28] and the moisture exchange on the cathode is properly organized, i.e., no pores are flooded, the fine pores in CG with the average diameter of tens of micron remain free of moisture. The latter is simply insufficient to fill the CG pores irrespective of whether the surface of these

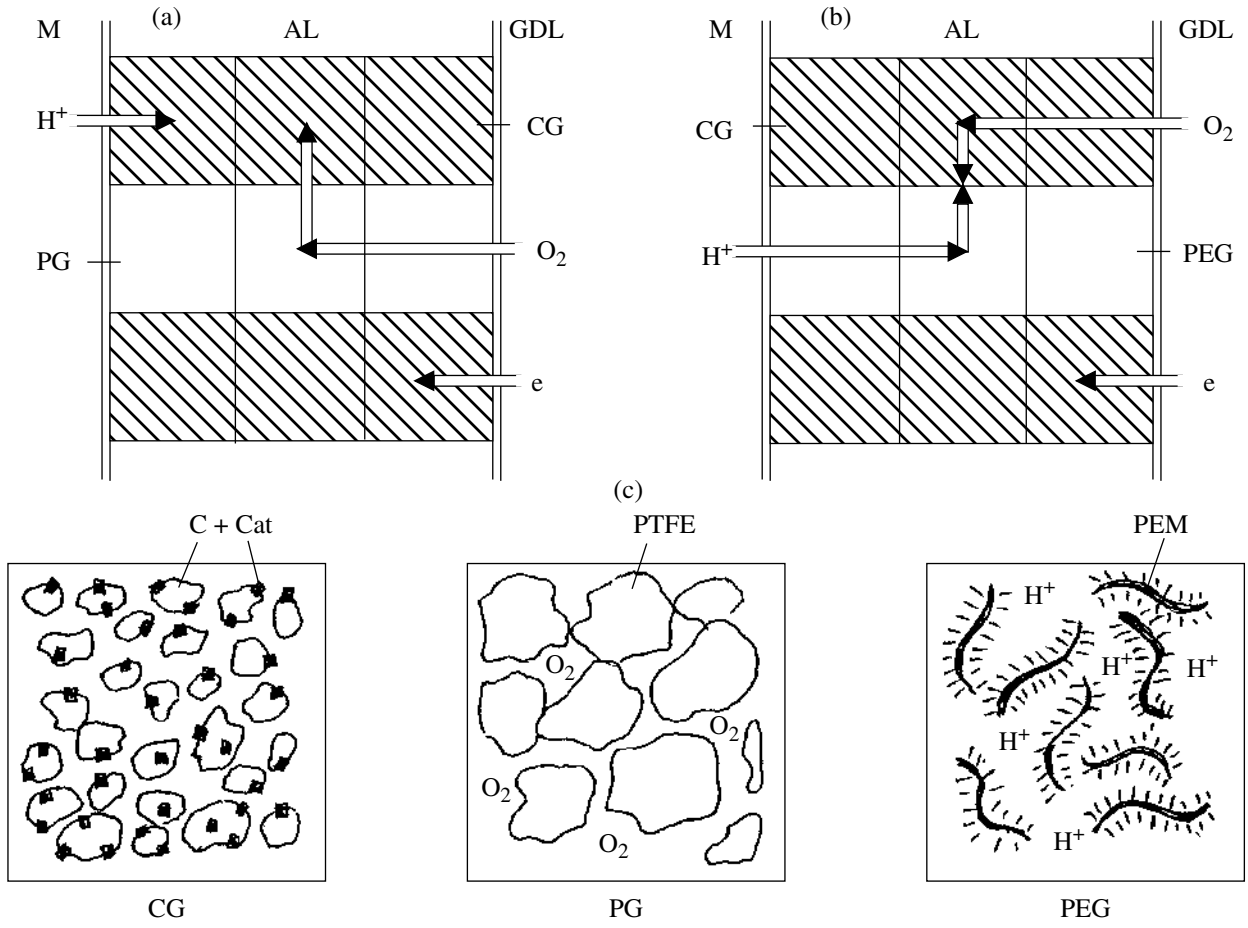

Fig. 5. Schematic illustration of channels for supplying electrons (e), protons (H^+), and oxygen molecules (O_2) into the active layer of (a) hydrophobized cathode and (b) cathode with Nafion within the framework of the "model of equidimensional grains", (c) conditional representation of the carrier, PTF, and Nafion grains. M is electrolyte chamber (hydrophobized cathode) or membrane (of Nafion) in a fuel cell. AL is active layer, GDL is gas-diffusion layer, CG is carrier (carbon black) grains with platinum catalyst, PG is PTE grains, NG is Nafion grains, CB is carbon black particles, C is catalyst particles, PEM are Nafion molecules.

pores is hydrophobic or hydrophilic. Hence, the oxygen delivery to the active layer proceeds via moisture-free pores in CG (Fig. 5b).

Yet another important remark should be made. In cathodes with Nafion, platinum localized in central parts of CG cannot take part in the electrochemical process. Due to the physicochemical nature of protonic conduction of a polymeric electrolyte, the current generation can occur only at the interface of the CG/PEG contact (Fig. 5b), where PEMs come into direct contact with Cat particles. This is why, on cathodes with Nafion, only a part of present catalyst can be involved in the current generation process.

Thus, as was shown in [9, 11], in a range of optimal concentrations of components (Nafion and carrier) in the active layer of a cathode with polymeric electrolyte, two kinds of three-dimensional percolation clusters with the fractal nature are formed. We call them the ionic (suppliers of protons, H^+) and the gas (suppliers of oxygen molecules, O_2, and electrons, e) clusters. Figure 5b shows a conventional picture of these clusters. On the other hand, in a hydrophibized electrode, an ionic cluster includes porous CG wetted with the liquid electrolyte (the channel for the delivery of protons and electrons into the current generation zone) and a gas cluster is built of porous electrolyte-free CG (the channel for the delivery of the gaseous reagent, Fig. 5a).

Hydrophobic pores in PG (Fig. 5c) have the average diameter of an order of magnitude of several tenth of μm; hence, in a gas cluster, the oxygen transfer occurs by the molecular diffusion mechanism. On the other hand, in an electrode with Nafion (Fig. 5b), a gas cluster consists of CG (the channel for the delivery of electrons and the gas), and its pores of the average diameter of

several tens nm are the location of the Knudsen diffusion (Fig. 5c).

The latter statement is principal and extremely important for understanding how the gas is actually delivered to the active layers of electrodes with Nafion. The concentration of voids in the active layer of such electrodes cannot be made substantial, otherwise the space free of CG and PEG is simply lost for the electrochemical process and the current on the cathode is low [11]. Moreover, it should be borne in mind that according to the percolation theory within the framework of the model of a lattice of sites [29] under study (Fig. 5), it is necessary that at least 30% of the cathode active layer volume was free of CG and PEG. It is unlikely for such a condition to be fulfilled. Thus, the presence of a small amount of voids in the cathode active layer is insufficient for the development of proper gas pores; this is why the gas in fact largely penetrates in the active layer via chains of porous CG (Fig. 5b).

In Figs. 5a and 5b, each of the ionic and gas clusters mentioned above is conditionally represented as a set of straight "rods" built of grains of the corresponding type. It should be stressed once more that electrons are delivered into the active layer in both hydrophobized electrodes and electrodes with Nafion via the chains of CG in contact with one another (via particles of conductive carbon black). Protons (we consider a hydrophobized electrode with an acidic electrolyte) travel in a hydrophobized cathode via the CG chains wetted with the liquid electrolyte and in an electrode with Nafion via PEG chains. The gas (oxygen) is supplied to the active layer in the electrode by PG chains (Fig. 5c), while in an electrode with Nafion, it is transported via CG chains, as was mentioned above.

Now, at last everything is ready for formulating the fundamental difference between mechanisms of operation of hydrophobized electrodes and electrodes with Nafion. In a hydrophobized electrode (Fig. 5a), oxygen molecules that move virtually without diffusion losses (the molecular diffusion coefficient of gases is large $D \sim 10^{-1}$ cm^2 s) via gas pores (chains of PG porous inside and free of moisture) are later dissolved in the electrolyte that fills CG (vertical arrow in Fig. 5a), diffuse there to ultimately take part in the electrochemical process.

Electrodes with Nafion operate differently (Fig. 5b). Here, as mentioned above, the current generation can occur only at the boundary between the gas and ionic clusters (the convergence point of vertical arrows in Fig. 5b). Although this boundary represents a kind of transition region from PEG to CG rather than a geometricall smooth plane, its thickness is very small (about several nm). Hence, in contrast to a gas-diffusion electrode (Fig. 5a), one can neglect the diffusion limitations on the delivery of oxygen into a zone where protons are encountered with electrons and oxygen.

Thus, this give rise to the qualitative difference in the mechanism of current generation in these two types of porous electrodes. In hydrophobized cathodes, we must first of all consider the process of gas diffusion from a gas pore in CG followed by its absorption there and only then take into account the Ohmic limitations on the ion delivery (Fig. 5a). On the other hand, in cathodes with Nafion, the processes of proton and gas delivery into the active layer to the surface of contact between the ionic and gas clusters turn out to be symmetrical (Fig. 5b); hence, here both the diffusion (oxygen supply) and Ohmic (supply of protons) limitations should be taken into account simultaneously.

In the theory of porous electrodes with a gaseous reagent, the efficiency of delivery of gas and ions into the active layer is known to play the key role in the current generation. Here we observe a paradoxic situation. In a hydrophobized cathode, virtually no limitations for the gas delivery to the active layer bulk exist and the specific conductivity of a liquid electrolyte in it is high, equal to approximately fractions of Ω^{-1} cm^{-1}. On the other hand, in a cathode with Nafion, limitations for the gas delivery into the active layer bulk are more severe, oxygen moves via fine pores in which the Knudsen diffusion coefficient $D \sim 10^{-3}$ cm^2/s and the optimal specific conductivity of Nafion $k \sim 0.1$ Ω^{-1} cm^{-1}. Insofar as the oxygen and proton transport proceeds in percolation clusters of complicated geometry, then according to estimates [9, 11], the effective values of the oxygen diffusion coefficient and protonic conductivity in an active layer prove to be smaller by an additional order of magnitude, namely, $D^* \sim 10^{-4}$ cm^2/s, $k^* \sim 0.01$ Ω^{-1} cm^{-1}.

Whereas it would seem that theoretical estimates confirm the fact that overall currents and power densities in a hydrophobized cathode should substantially exceed the corresponding values in a cathode with Nafion, the practice (experiments) evidences the opposite, namely, the overall characteristics of cathodes with Nafion much exceed their counterparts in a hydrophobized cathodes with liquid electrolytes. Hence, it can be assumed that in fuel cells with polymeric electrolytes, some different factor operates that makes them advantageous over the fuel cells of other types. The rapid increase in the overall current with an increase in overpotential is precisely such a factor. Let us demonstrate this.

COMPARING VOLTAMMETRIC CHARACTERISTICS OF HYDROPHOBIZED CATHODE AND ELECTRODES WITH NAFION

Now we set a task to relate the overall current to the overpotential for a hydrophobized cathode and a cathode with polymeric electrolyte.

Hydrophobized cathode. Here, following the directions given in Fig. 5a, the calculations of a voltammetric characteristic should be started with calculating the current i generated in a volume unit of the cathode active layer in an arbitrary section y, where y is the coordinate that is normal to the frontal surface of the active layer (M/AL interface) and is reckoned from it. According to [13], the gas diffusion to the electrolyte that fills the carrier grains, followed by the electrochemical discharge in the vicinity of a gas pore in the form of a cylinder is described by the equation

$$(1/\rho^*)d\rho^*(d\acute{c}/d\rho^*)/d\rho^* = \acute{c} - \exp(-2\eta), \quad (9)$$

where $\acute{c} = c/c_o$ is the electrolyte supersaturation with the gas, c_o is the gas solubility, η is the normalized cathodic overpotential

$$\eta = (E^{st} - E)/b. \quad (10)$$

where E is the cathode potential, E^{st} is the steady-state potential, b is the Tafel plot slope, $\rho^* = \rho/L_d$ is the normalized radius, L_d is the characteristic diffusion length

$$L_d = (nFD\nu c_o/j\lambda)^{1/2}\exp(-\eta/2) = L^0_{d,m}\exp(-\eta/2), \quad (11)$$

where n is the number of electrons involved in an elementary act, D is the oxygen diffusion coefficient in electrolyte solution, ν is the carrier grain porosity, j is the current density generated in carrier grains containing catalyst.

Equation (9) should be supplemented with boundary conditions

$$\acute{c}|_{\rho = d/2} = 1 \quad d\acute{c}/d\rho|_{\rho = L} = 0, \quad (12)$$

where L is a half of the average distance between neighboring gas pores.

Solving Eq. (9) with boundary conditions (12), we obtain the following expression for the current density J per surface unit of a gas pore:

$$J = (nFD\nu c_o j\lambda)^{1/2}\exp(\eta/2)[1 - \exp(-2\eta)]\psi, \quad (13)$$

where

$$\psi = \{I_1(L/L_d)K_1(d/2L_d) - I_1(d/2L_d)K_1(L/L_d)\}/\{I_1(L/L_d)K_0(d/2L_d) + I_0(d/2L_d)K_1(L/L_d)\}, \quad (14)$$

and I_0, I_1, K_0, K_1 are Bessel functions of a purely imaginary argument.

Now, we determine the expression for the bulk current density i. It can be shown [13] that in the model of cylindrical gas pores under consideration, the i value is the product of two cofactors

$$i = 3\pi d(1/2L)^2(nFD\nu c_o j\lambda)^{1/2}\exp(\eta/2) \times [1 - \exp(-2\eta)]\psi = \varepsilon\varphi(\eta). \quad (15)$$

For the further calculations, it is necessary to elucidate the dependence of i on the overpotential η. According to Eq. (15),

$$i \sim \varphi = \exp(\eta/2)[1 - \exp(-2\eta/)]\psi. \quad (16)$$

Thus, in the first approximation, we can assume that $i \sim \mathrm{Exp}(\eta/2)$.

Now, we take into account the Ohmic limitations. The overpotential distribution over the thickness of a hydrophobized electrode is described by the equation

$$d^2\eta/d\ddot{y}^2 = \varphi(\eta), \quad (17)$$

where $\ddot{y} = y/L_{Ohm}$ is the normalized coordinate. The characteristics Ohmic length

$$L_{ohm} = (bk^*/\varepsilon)^{1/2}, \quad (18)$$

Here, k^* is the effective specific ionic conductivity in the active layer. Equation (17) should be supplemented by boundary conditions

$$\eta|_{y = 0} = \eta_0 = (E^{st} - E_0)/b, \quad d\eta/dy|_{y = \Delta} = 0, \quad (19)$$

where E_0 is the cathode potential, Δ is its thickness. The overall cathodic current I is determined by the expression

$$I/I_{ohm} = 2^{1/1}\left[\int_{\eta_\Delta}^{\eta_0}\varphi(\eta)d\eta\right]^{1/2}, \quad (20)$$

where the characteristic Ohmic current

$$I_{ohm} = (bk^*\varepsilon)^{1/2}. \quad (21)$$

Thus, ultimately, the sought dependence of the overall current on the overpotential in hydrophobized cathodes that takes into account Eqs. (16) and (20) has the form

$$I \sim \varphi^{1/2} \sim \exp(\eta_0/4). \quad (22)$$

Cathode with Nafion. Taking into account symmetry of the processes of delivery of protons and oxygen molecules into the current generation zone (to the surface of contact between ionic and gas clusters, Fig. 5b), we have the following conditions for calculating the overall current [18]. The distribution of the normalized

overpotential η in the active layer of an oxygen cathode is now determined by the equation

$$d^2\eta/d\hat{y}^2 = \acute{c}e^{\eta} - e^{-\eta}, \quad (23)$$

where $\hat{y} = y/L_{ohm}$ is the normalized coordinate. The characteristic Ohmic length

$$L_{ohm} = (bk^*/Si_o)^{1/2}, \quad (24)$$

where S is the specific surface of platinum accessible for the electrochemical process, i_0 is the exchange current. Equation (23) should be supplemented by limiting conditions (19).

The distribution of the Nafion oversaturation with oxygen in the active layer is now determined by the expression similar to Eq. (23)

$$d^2\acute{c}/d\hat{y}^2 = \Omega[\acute{c}\, e^{\eta} - e^{-\eta}], \quad (25)$$

Where parameter $\Omega = (L_{ohm}/L_d)^2$, and L_d is the characteristic diffusion length determined by the expression

$$L_d = (nFD^*c_o/Si_0)^{1/2}, \quad (26)$$

where D^* is the effective coefficient of gas diffusion in the cathode active layer. Equation (25) should be supplemented by boundary conditions. For an oxygen cathode,

$$y = 0 \;\; d\acute{c}/d\acute{y} = 0 \quad y = \Delta \;\; \acute{c} = 1. \quad (27)$$

Then, the overall current on the cathode with Nafion can be obtained as a result of simultaneous solution of the system of equations (23) and (25) with boundary conditions (19) and (27). This overall current

$$I = -I_{ohm}d\eta/d\hat{y} \quad \text{for } y = 0, \quad (28)$$

where the characteristic current

$$I_{ohm} = (bk^*Si_0)^{1/2}. \quad (29)$$

Now, we elucidate the form of the I dependence on the cathodic overpotential η_0. Let us consider the following two limiting cases: 1) parameter $\Omega \ll 1$, and the limitations on the gas delivery to the current generation zone can be neglected and 2) parameter $\Omega \gg 1$, and the limitations on the proton delivery to the current limitation zone can be neglected.

Case 1. Here (for $\Omega \ll 1$), the gas oversaturation in the active layer $\acute{c}$ can be assumed identically equal to 1. Then, in place of Eq. (23), we obtain equation

$$d^2\eta/d\hat{y}^2 = 2\mathrm{sh}\,\eta. \quad (30)$$

Integrating Eq. (30) with conditions (19) taken into account gives the following expression for the overall current:

$$I = 2I_{ohm}(\mathrm{ch}\,\eta_0 - \mathrm{ch}\,\eta_\Delta)^{1/2}, \quad (31)$$

where η_Δ is the cathode overpotential on the back side of the active later. Insofar as the inequality $\eta_0 \gg \eta_\Delta$ is usually true under working conditions, then the following condition is true ultimately:

$$I \sim \exp(\eta_0/2). \quad (32)$$

Case 2. Here, the cathode overpotential in the active layer can be taken constant and equal to η_0. In this case, we integrate Eq. (25) and eliminate the second term on the right. As a result, we obtain the following expression for the overall current:

$$I = I_d\mathrm{th}[\Delta\exp(\eta_0/2)/L_d], \quad (33)$$

where the characteristic diffusion current

$$I_d = (nFDc_oSi_0)^{1/2}\exp(\eta_0/2). \quad (34)$$

Because as the cathodic potential η_0 increases, the term $\mathrm{th}[\Delta\exp(\eta_0/2)/L_d]$ quickly becomes equal to 1, and we are again convinced that at $\Omega \gg 1$ as well, the overall current increases according to a law expressed by formula (32).

More detailed calculations show that for a cathode with Nafion, formula (32) remains true also when the characteristic Ohmic and diffusion lengths are commensurable, when $\Omega \sim 1$.

Thus, comparison of Eqs. (22) and (32) suggests that with the increase in overpotential, the overall current in electrodes with Nafion increases more quickly as compared with hydrophobized electrodes. This also explains the well-known fact that fuel cells with Nafion have high power characteristics as compared with fuel cells of other types (particularly, those with phosphoric-acid and alkaline fuel cells).

These general reasoning should be substantiated by concrete estimates. Assume for sake of simplicity that in a hydrophobized cathode and a cathode with Nafion, all parameters characterizing the polarization curves of the oxygen reduction and the oxygen and proton delivery are the same. Assume that in this case, the steady-state potential $E^{st} = 1.05$ V and the polarization curve slope is 60 mV (this means that $b = 2.6 \times 10^{-2}$ V). Then, at a potential $E_0 = 0.8$ V, according to Eq. (22), the current increases by a factor $\exp[(E^{st} - E_0)/4b] = \exp[2.4] = 11$ in a hydrophobized cathode and by a factor of $\exp[(E^{st} - E_0)/2b] = \exp[4.8] = 121$ in a cathode with Nafion. At $E_0 = 0.6$ V, the difference in the current increments will be still more pronounced. Now, the current increases 76-fold in a hydrophobized cathode and $(76)^2 = 5776$-fold in a cathode with Nafion. And in place of the 11-fold current lag of a hydrophobized cathode over a cathode with Nafion, we have the 76-fold lag.

CONCLUSIONS

The results of calculations of the main overall characteristics of both an individual cathode and the whole

Designations for parameters characterizing a fuel cell with Nafion and platinum and their values taken in calculations

t = 60, 80 and 95°C is the fuel cell temperature

p*= 101 and 505 kPa is the pressure in the gas chamber

E_{st} = 1.05 V is the steady state potential of cathode

E* = 0.825 V is the break point potential in the polarization curve

$b_1 = 2.6 \times 10^{-2}$ V is the Tafel plot slope in the high potential range

$b_2 = 5.2 \times 10^{-2}$ V is the Tafel plot slope in the low potential range

n = 4 is the number of electrons involved in the electrochemical reaction

$F = 9.6 \times 10^4$ C/mol is the Faraday number

$i_0 = 10^{-8}$ A/cm^2 is the exchange current in the high potential range at t = 50°ë

d = 100 nm is the average size of Nafion and carrier grain edges

d_s = 30 nm is the average pore size in carrier grains

g_e = 0.5 is the volume concentration of Nafion grains

g_s = 0.5 is the volume concentration of carrier grains

g_0 = 0 is the volume concentration of grains-voids

g_w = 20 mass % is the platinum content in carrier grains

i* is the characteristic bulk current density in the high potential range (to be calculated)

$D^* = 4.5 \times 10^{-4}$ cm^2/s is the effective diffusion coefficient of oxygen in Nafion in the active layer

$S^* = 1.33/L = 1.33 \times 10^5$ cm^{-1} is the specific surface of the contact between the ionic and gas clusters at $g_e = g_s = 0.5$

$S = S^*\mu\xi = 1.33 \times 10^5$ cm^{-1} is the specific surface of platinum particles that can take part in the electrochemical process

$C_0 = 5 \times 10^{-6}$ g-mol/cm^3 is the oxygen solubility in Nafion at p*= 101 kPa

Δ = 1, 3 and 10 μm is the active layer thickness

δ is the thickness of the Nafion membrane (this parameter is varied)

ν = 0.5 is the porosity of carrier grains

$k = 1 \times 10^{-1}$ Ω^{-1} cm^{-1} is the specific conductivity of Nafion

$k^* = 1.09 \times 10^{-2}$ Ω^{-1} cm^{-1} is the effective specific conductivity of Nafion in the active layer

ξ = 5 is the factor of "fuzziness" of the contact surface between the ionic and gas clusters

μ = 0.2 is the electrochemical roughness factor

hydrogen–oxygen (air) fuel cell with Nafion and platinum are demonstrated. It is analyzed how the overall characteristics of such fuel cells depend on the variations in the main parameters of both the active layer and a membrane made of a solid polymeric electrolyte. These calculations demonstrate the correctness of the "model of equidimensional grains", the ability of this model of the cathode active layer to adequately describe the processes that really occur in hydrogen–oxygen (air) fuel cells with Nafion and platinum.

The overall characteristics of hydrogen–oxygen (air) fuel cells with solid polymeric electrolytes are compared with those of fuel cells with hydrophobized cathodes and a liquid electrolyte. The conditions for the supply to active layers of hydrophobized cathodes are much more favorable as compared with cathodes with a solid polymeric electrolyte (Nafion). However, the current in cathodes with Nafion increases more actively with an increase in overpotential (the current increases ~ Exp[η_0/2], where η_0 is the cathodic overpotential) as compared with hydrophobized cathodes (here, the current ~ Exp[η_0/4]]). This is the decisive factor. It explains the experimentally observed fact that fuel cells with Nafion demonstrate higher current and power characteristics as compared with fuel cell of other types.

REFERENCES

1. Costamagna, P. and Srinivasan, S. *J. Power Sources*, 2001, vol. 102, p. 242.
2. Springer, T.E. and Gottesfeld, S, *Modeling of Batteries and Fuel Cells*, White, R.E., Verbrugge, M.W., and Stockel, J.F, Eds., The Electrochemical Society Proceedings Series, New York: Pennington, 1991, PV 91-10, P. 197.
3. Gottesfeld, S. and Zawodzinski, T.A., *Advances in Electrochemical Science and Engineering*, Tobias, C. N. Y., Ed., New York: Wiley, 1997, vol. 5.
4. Perry, M.I., Newman, J., and Cairns, E.J., *J. Electrochem. Soc.*, 1998, vol. 145, p. 5.

5. Eikerling, M. and Kornyshev, A.A., *J. Electroanal. Chem.*, 1998, vol. 453, p. 89.
6. Wang, C.Y., *Chem. Rev.*, 2004, vol. 104, p. 4727.
7. Weber, A.Z. and Newman J., *Chem. Rev.*, 2004, vol. 104, p. 4679.
8. Mukherjee, P. and Wang, C.-Y., *J. Electrochem. Soc.*, 2006, vol. 153(5), p. A840.
9. Chirkov, Yu.G. and Rostokin, V.I., *Elektrokhimiya*, 2004, vol. 40, p. 1036.
10. Chirkov, Yu.G. and Rostokin, V.I., *Elektrokhimiya*, 2005, vol. 41, p. 1109.
11. Chirkov, Yu.G. and Rostokin, V.I., *Elektrokhimiya*, 2006, vol. 42, p. 799.
12. Chirkov, Yu.G. and Rostokin, V.I., *Elektrokhimiya*, 2007, vol. 43, p. 827.
13. Chirkov, Yu.G. and Rostokin, V.I., *Elektrokhimiya*, 2007, vol. 43, p. 154.
14. Damjanovic, A., Genshaw, M.A., and Bockris J.O.`M., *J. Phys. Chem.*, 1966, vol. 45, p. 4057.
15. Sepa, D.B., Vojnovic, V., and Damjanovic, A., *Electrochim. Acta*, 1981, vol. 26, p. 781.
16. Parthasarathy, A., Srinivasan, S., and Appleby, J., *J. Electrochem. Soc.*, 1992, vol. 139, p. 2530.
17. Antoine, O., Bultel, Y., and Durand, R., *J. Electroanal. Chem.*, 2001, vol. 499, p. 85.
18. Chirkov, Yu.G. and Rostokin, V.I., *Elektrokhimiya,* 2006, vol. 42, p. 806.
19. Mitsushima, S., Araki, N., Kamiya, N., and Ota, K., *J. Electrochem. Soc.*, 2002, vol. 149, p. A1371.
20. Parthasarathy, A., Srinivasan, S., Appleby, A.J., and Martin, C.R., *J. Electrochem. Soc.*, 1992, vol. 139, p. 2530.
21. Uchida, M., Aoyama, Y., Eda, N., and Ohta, A., *J. Electrochem. Soc.*, 1995, vol. 142, p. 4143.
22. Gode, P., Lindbergh, G., and Sundholm, G., *J. Electroanal. Chem.*, 2002, vol. 518, p. 115.
23. *Handbook of Fuel Cells – Fundamentals, Technology and Applications*, vol. 1, Wiley, 2003. p. 42.
24. Wilkinson, D.P., and Steck A.E., *Proc. Second International Symposium on New Materials for Fuel Cell and Modern Battery Systems*, Savadogo, O., Roberge, P.R., Eds., Montreal: Ecole Polytechnique de Montreal, 1997, p. 27.
25. *Handbook of Fuel Cells – Fundamentals, Technology and Applications*, vol. 3, Wiley, 2003, p. 593.
26. *Handbook of Fuel Cells – Fundamentals, Technology and Applications*, vol. 1, Wiley, 2003, p. 566.
27. Neyerlin, K.C., Gu, W., Jorne, J., and Gasteiger, H.A., *J. Electrochem. Soc.*, 2006, vol. 153, p. A1955.
28. Costamagna, P., and Srinivasan, S., *J. Power Sources*, 2001, vol. 102, p. 253.
29. Chirkov, Yu.G., *Elektrokhimiya*, 1999, vol. 35, p. 1449.

SPELL: ok